Mol Cell Biochem (2012) 359:217–223
DOI 10.1007/s11010-011-1016-x

Hepatic stellate cells produce vascular endothelial growth factor via phospho-p44/42 mitogen–activated protein kinase/cyclooxygenase-2 pathway

Yi Zhao · Yanqing Wang · Qiang Wang · Zhengrong Liu · Qingfeng Liu · Xin Deng

Received: 21 April 2011 / Accepted: 27 July 2011 / Published online: 24 August 2011

Abstract Vascular endothelial growth factor (VEGF) is one of the major cytokines secreted by activated hepatic stellate cells (HSCs). VEGF is involved in hepatic angiogenesis and plays an important role in the development of liver fibrosis. TNP-470, an angiogenic inhibitor, attenuates the development of rat liver fibrosis with reduced angiogenesis, as demonstrated in our previous study. HSCs were prepared from specific pathogen-free Wister rat livers. The isolated HSCs were activated and stimulated with platelet-derived growth factor BB (PDGF-BB) or prostaglandin E_2 with or without pretreatment with MAPK cascade inhibitors (PD98059, which inhibits MEK activation), SB203580 (a selective pharmacologic inhibitor of p38 MAPK), and SP600125 (a selective inhibitor of the c-Jun N-terminal kinase, JNK). VEGF production and those of related molecules were assayed at the protein and mRNA levels by immunostaining, western blot analysis, and real-time quantitative PCR. The activated HSCs produced more VEGF than the quiescent ones. Those that received PDGF-BB stimulation showed enhanced cyclooxygenase-2 (COX-2) expression and activation of phosphor-mitogen-activated protein kinase (MAPK) p44/p42. Pretreatment with PD98059 significantly inhibited COX-2 expression and VEGF production within the PDGF-activated HSCs, but the effect was nullified by exogenous prostaglandin E_2. pJNK and p38 inhibitors do not show similar inhibitory effects on VEGF and COX-2 expression, and pJNK and p38 MAPK signals are not involved in the COX-2/MAPK signaling cascade. VEGF production in PDGF-stimulated HSCs is dependent on the overexpression of COX-2 protein via the phospho-p42/44 MAP kinase activation, based on PD98059 inhibition.

Keywords Activated hepatic stellate cells · Platelet-derived growth factor BB · Vascular endothelial growth factor · Cyclooxygenase-2

Introduction

Hepatic stellate cells (HSCs) are a major regulator in liver homeostasis and play a central role in the response to liver injury. Activated HSCs proliferate and produce a large amount of extracellular matrix materials, leading to liver fibrosis [1]. Platelet-derived growth factor (PDGF) is the most potent mitogen for HSCs in culture. The binding of PDGF to PDGF receptor-β (PDGFR-β) recruits a signaling molecule called Ras, which leads to the activation of the mitogen-activated protein kinase (MAPK) cascade. Some cytokines are then sequentially produced to modulate metabolism and homeostasis in mesenchymal cells [2]. PDGF may increase the synthesis of cyclic adenosine monophosphate (cAMP) to evoke prostaglandin (PG)/cAMP signals, which leads to cyclooxygenase-2 (COX-2) activation [3–6]. Therefore, the MAPK and COX-2/PG pathways have major effects on the activation of HSCs.

Vascular endothelial growth factor (VEGF) is an approximately 34- to 46-kDa homodimeric glycoprotein. It has eight polypeptide-encoding exons and includes several

Yi Zhao and Yanqing Wang contributed equally to this study.

Y. Zhao (✉) · Q. Wang · X. Deng
Department of Gastroenterology Surgery, Affiliated Shengjing Hospital, Medical University of China, 36 Sanhao Street, Heping District, Shenyang, China
e-mail: zhaoyi_zhao@126.com

Y. Wang · Z. Liu · Q. Liu
Center for the Study of Liver Disease and Department of Surgery, Liaoning Province Hospital, Shenyang 110042, China

splice variants with 121, 145, 165, 189, and 206 amino acid residues [7–10]. $VEGF_{121}$ is encoded by exons 1–5 and 8; $VEGF_{145}$ and $VEGF_{165}$ are added by exons 6 and 7, respectively; and $VEGF_{189}$ and $VEGF_{206}$ both contain peptides encoded by exons 6 and 7 [11]. $VEGF_{121}$, $VEGF_{145}$, and $VEGF_{165}$ induce the proliferation of endothelial cells and regulate blood vessel formation [12]. In the liver, VEGF can be overexpressed in a variety of conditions, such as injury, regeneration, and carcinoma [13–15]. It is probably due to the action of VEGF, which causes highly vascularized, well-developed fibrous septa to form, a salient pathologic characteristic of liver cirrhosis [16]. One of our previous studies demonstrated that TNP-470 (an angiogenic inhibitor) attenuates the development of rat liver fibrosis with reduced angiogenesis [17]. A recent report revealed that the interaction between VEGF and its receptor is a prerequisite for murine hepatic fibrogenesis [18]. Another report showed that activated HSCs produce VEGF protein and thereby play a proangiogenic role in melanoma metastasis [15]. These results suggest that VEGF is one of the major cytokines secreted by HSCs. VEGF is involved in hepatic angiogenesis and plays an important part in the development of liver fibrosis.

The PI3K/Akt pathway is also activated following PDGF stimulation of HSCs. Studies confirm that activation of PI3K is important for HSC proliferation and chemotaxis. Inhibition of PI3K by wortmannin blocks mitogenesis in response to PDGF, supporting the involvement of this pathway in HSC proliferation [29]. Inhibition of PI3K with wortmannin also reduces ERK activity and c-Fos mRNA levels, suggesting that cross-talk occurs between the PI3K and MAPK pathways following PDGF stimulation in HSCs [30]. So, we also investigated the effects of inhibitors of PI3K/Akt pathway on the VEGF regulation by using a more specific PI3K inhibitor, LY294002.

In the current study, to clarify the regulatory mechanism of VEGF production in activated HSCs using a comparative method, we measured PDGF-BB-stimulated VEGF production with or without pretreatment with MAPK cascade inhibitors (PD98059, which inhibits MEK activation), SB203580 (a selective pharmacologic inhibitor of p38 MAPK), and SP600125 (selective inhibitor of c-Jun N-terminal kinase, JNK) [19–21].

Materials and methods

Animals

Specific pathogen-free male Wister rats were purchased from the Experimental Center of Liaoning Province Hospital. They were fed a diet of standard chow pellets and water ad libitum. All animals were handled in accordance with the standard guidelines for animal experiments of Experimental Center of Liaoning Province Hospital, China.

Isolation and culture of HSCs

Stellate cells were prepared from the rat liver as previously described [17]. Under ether anesthesia, the abdomen was opened. The liver was perfused via the portal vein first with Krebs–Ringer solution, pH 7.3, for 10 min at 37°C and then with Krebs–Ringer solution containing 0.08% pronase E (Merk, Darmstadt, Germany) and 0.04% collagenase (Wako Pure Chemical Co., Osaka, Japan) for 30 min at 37°C at the rate of 10 mL/min. The liver was taken out, cut into small pieces, and incubated in Krebs–Ringer solution containing 0.05% pronase E, 0.05% collagenase, and 20 μg/mL of deoxyribonuclease (Boehringer, Mannheim, Germany) for 30 min at 37°C. Cell suspension was filtered through a 150-μm mesh. After centrifugation in an 8.2% Nycodenz cushion (Nycomed Pharma AS, Oslo, Norway) at 1,400*g* for 20 min at 4°C, a stellate cell–enriched fraction was obtained from an upper whitish layer. Cells were washed by centrifugation (400*g*, 4°C, 10 min) and cultured in RPMI 1640 (Gibco, Grand Island, NY) supplemented with 5% fetal bovine serum (FBS; Gibco) and antibiotics (105 U/L penicillin G and 100 mg/L streptomycin). The purity was more than 95%.

The HSCs were obtained from livers and then isolated. These cells were suspended in Dulbecco's modified Eagle's medium (DMEM; Gibco Laboratories, Grand Island, NY) with 10% fetal bovine serum (FBS; Gibco Laboratories) at a cell density of 5×10^5 cells/mL with antibiotics (0.035 g/L penicillin and 100 mg/L streptomycin). The purity of HSCs was above 95% and the viability was above 90%, which were evaluated with the Trypan blue exclusion test [17].

The activated HSCs were obtained through a 1-week culture of fresh isolated HSCs in 10% FBS–DMEM and used after starvation for 24 h with 0.5% FBS–DMEM. α-SMA and desmin immunostaining was performed to confirm that the cells are activated HSCs. They were then incubated with 10 ng/mL PDGF-BB or 10 μmol of PGE_2 for 0.25, 0.5, 3, 6, and 9 h with or without separate pretreatment with 12 μmol PD98059 (sc-3532; Santa Cruz Biotechnology, Inc., Santa Cruz, CA), 10 μmol SB203580 (sc-3533; Santa Cruz Biotechnology), 50 μmol SP600125 (Sigma Chemical, Co.), and 20 μmol Ly294002 (Sigma Chemical Co.) for 0.5 h in serum-free medium.

Immunostaining of cultured cells

HSCs cultured with 10% FBS–DMEM were stained with monoclonal antibodies against α-smooth muscle actin (α-SMA; 1:100 dilution; Sigma Chemical, Co.), desmin

(1:50 dilution; Dako, Osaka, Japan), and VEGF (1:200 dilution; Santa Cruz Biotechnology, Inc.,) [17]. Five microscopic fields were counted. The percentage of positive cells was then calculated. The experiments were repeated three times.

Western blot analysis

The activation of phospho-p44/42 MAPK was measured using the MAPK assay kit (Cell Signaling Technology, Inc., Beverly, MA) in line with the manufacturer's protocol. The sodium dodecyl sulfate (SDS) sample buffer (62.5 mM Tris–HCl [pH 6.8 at 25°C], 2% w/v SDS, 10% glycerol, 50 mM DTT, and 0.01% bromophenol blue or phenol red) was added to the culture. The cells were immediately scraped off the plate, and the extract was transferred to a microcentrifuge tube and kept on ice. The samples were denatured at 95°C for 5 min after 10–15 s of sonication. The protein samples were fractionated through 5–10% SDS–polyacrylamide gel electrophoresis and transferred onto polyvinylidene difluoride membranes. After washing, the membrane was treated with 5% skimmed milk at room temperature for 1 h and incubated overnight with mouse monoclonal antibodies against β-actin (1:5,000 dilution; Sigma Chemical, St. Louis, MO) and pJNK (clone G7) (1:1,000 dilution; Santa Cruz Biotechnology), rabbit polyclonal antibodies against cyclooxygenase-2 (COX-2) (1:1,000 dilution; Santa Cruz Biotechnology), VEGF (1:1,000 dilution; Santa Cruz Biotechnology), and p38 (1:1,000 dilution; Santa Cruz Biotechnology), rabbit polyclonal antibodies against phospho-p44/42 MAPK (1:1,000 dilution) and p44/42 MAPK (1:1,000 dilution), respectively, at 4°C. The membrane was then washed and incubated with horseradish peroxidase–conjugated anti-rabbit antibodies (1:2,000 dilution; Dako) against VEGF, COX-2, p38, phospho-p44/42 MAPK, and p44/42MAPK or anti-mouse antibodies against β-actin at room temperature for 1 h. After the second washing, the immunoreactive bands were visualized on an X-ray film using ECL detection (Amersham Bioscience, Arlington Heights, IL). The density of bands was quantified through laser densitometer (ATTO densitograph 4.0), and the mean value was calculated from three independent experiments.

Real-time quantitative polymerase chain reaction

The RNA extracted from the fresh cellular samples was used for first-strand complementary DNA synthesis (Roche Molecular Systems, Inc., Alameda, CA). For real-time qPCR, an ABI PRISMTM 7700 Sequence Detection System (Applied Biosystems) was used. The COX-2 primer (5′-FAM-CTTTGC CCAGCAC TTCACC CATCAG TT–TAMRA-3′), The sequences of the primer were $VEGF_{165}$(S) (5′-AGCGGA GAAAGC ATTTGT TTG-3′) and $VEGF_{165}$(AS) (5′-CAACGC GAGTCT GTTTTG-3′). The VEGF probe (5′-FAM-CCAAGATCCG CAGACGTG TA AATGTTCC–TAMRA-3′), the HPLC-graded sense primer (5′-AGCGGAGAAA GCATTTGTTTG-3′), and the antisense primer (5′-CAACGCGAGT CTGTGTTTTG-3′) were designed by ABI PRISM® Primer Express Software (Applied Biosystems) according to the manufacturer's instructions. The conditions were as follows: 50°C for 2 min, 95°C for 10 min, and 40 cycles of 95°C for 0.5 min and 60°C for 1 min.

Statistics

The data are presented as means ± standard error of means (SEM). Analyses of the effects of various treatments were conducted using one-way ANOVA and a two-tailed t test. P values less than 0.05 were considered statistically significant.

Results

VEGF overexpression in activated HSCs

The HSCs were isolated and cultured for 1 day (quiescent cells) and 7 days (activated cells) with 10% FBS–DMEM. The α-SMA-positive and desmin-positive HSCs were representatives of activated cells, which has been demonstrated in our previous study [17]. The results show that the proportion of activated HSCs (7 days) positive for α-SMA, desmin, and VEGF to the total HSCs increased compared with the quiescent HSCs from 1.1, 5.8, and 4.5% (16 h) to 37.6, 48.9, and 19.6% (7 days), respectively (Fig. 1).

PDGF induces expression of COX-2 and phospho-p44/42 MAPK, which precedes VEGF production in activated HSCs

The kinetics after stimulation with PDGF-BB was investigated. The activated HSCs were cultured with PDGF-BB (10 ng/mL) for 0.25, 0.5, 3, 6, and 9 h in serum-free DMEM. The results show that PDGF-BB induced the overexpression of COX-2 protein, which reached the peak up to 11.2-fold at hour 3 compared with the control ($P < 0.01$, $n = 3$), and activation of phospho-p44/42 MAPK, which was concurrently enhanced up to the peak at min 30, which preceded the VEGF peak at hour 6, reaching 6.96-fold (p44), 5.81-fold (p42), and 10.9-fold compared with the MAPK or the control, respectively (Fig. 2) ($P < 0.01$, $n = 3$).

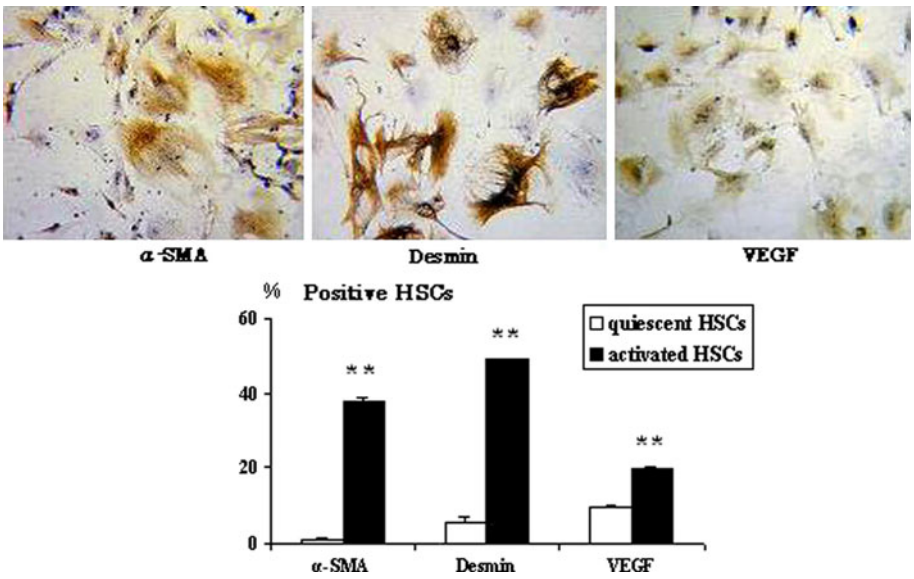

Fig. 1 VEGF production consistent with HSC activation. The percentage of α-SMA-desmin-positive and VEGF-positive HSCs to the total HSCs cultured with 10% FBS–DMEM for 16 h and 7 days, respectively. The value represents the activated HSCs (7 days) compared with the quiescent HSCs (16 h). Data represent the mean ± SEM. $n = 3$, $^{**}P < 0.01$

PDGF induces pJNK and p38 upregulation in activated HSCs

The activated HSCs were cultured with PDGF-BB (10 ng/mL) for 0.25, 0.5, 3, 6, and 9 h in serum-free DMEM. The expression of pJNK and p38 was detected with western blot analysis and reverse transcriptase PCR. The results show that PDGF-BB induced the upregulation of pJNK and p38, which concurrently rose at min 30 and reached the peak at up to 11.2-fold at hour 3 compared with the control (Fig. 3) ($P < 0.01$, $n = 3$).

VEGF is produced from activated HSCs by PDGF-BB via COX-2/PGE_2 pathway

To reveal the regulatory mechanism of VEGF production by activated HSCs, we induced HSCs activation by 10 ng/mL PDGF-BB, with or without pretreatment with 12 μmol PD98059, 10 μmol SB203580, 50 μmol SP600125, and 20 μmol Ly294002. We measured VEGF and COX-2 expression with serum-free DMEM for 3 h by western blot analysis (Fig. 4a) and real-time quantitative PCR (Fig. 4b). Among them, only PD98059 compounds were able to suppress COX-2 and VEGF expression in the PDGF-BB–activated HSCs. These results suggested that COX-2 is the downstream target of phospho-p44/42 MAPK for VEGF production in activated HSCs stimulated by PDGF signal transduction. In addition, pJNK and p38 inhibitors did not demonstrate similar inhibitory effects on VEGF and COX-2 expression. The pJNK and p38 MAPK signals were not involved in the COX-2/MAPK signaling cascade, leading to VEGF production in the PDGF-BB–activated HSCs, and PI3K/Akt pathway did not interfere with the COX-2/VEGF pathway in activated HSC ($P < 0.05$, $n = 3$). Additionally, the COX-2–dependent inhibitory events could be superseded by exogenous inoculation with PGE_2, and VEGF production could be rapidly rescued (peak at hour 3) in a time-dependent manner. Despite pretreatment with PD98059, there was no apparent inhibitory effect on VEGF production (Fig. 4c). Our previous study has demonstrated that directly blocked Cox-2 will reduce the expression of VEGF in a dose-dependent manner [5].

Discussion

In liver injury associated with tissue remodeling, activated stellate cells are accumulated by migrating to the sites of necrotic damage, producing abundant extracellular matrix materials that lead to post-necrotic fibrosis. Several factors influence the proliferation and activation of HSCs [1, 22]. Among them, PDGF-BB, a potent mitogen for cultured stellate cells, potentially augments stellate cell migration and promotes HSCs to produce and secrete VEGF protein [15, 16]. VEGF induces angiogenesis to restore the microvascular network for the delivery of oxygen and nutrients to the healing site [23, 24]. The VEGF protein produced by activated HSCs is believed to play a key role in angiogenesis and fibrogenesis in the injured liver [1]. In our earlier study, TNP-470 antiangiogenesis factor was shown to suppress HSC activation and subsequent vascularization in injured liver [17]. A recent study also demonstrated that specific neutralizing monoclonal antibodies (R-1mAb and R-2mAb) that inhibit VEGF receptor-1 and VEGF receptor-2 significantly attenuated the development of fibrosis associated with suppression of neovascularization in injured liver [11]. Recent reports also demonstrated that COX-2 inhibitors attenuated hepatic fibrosis by

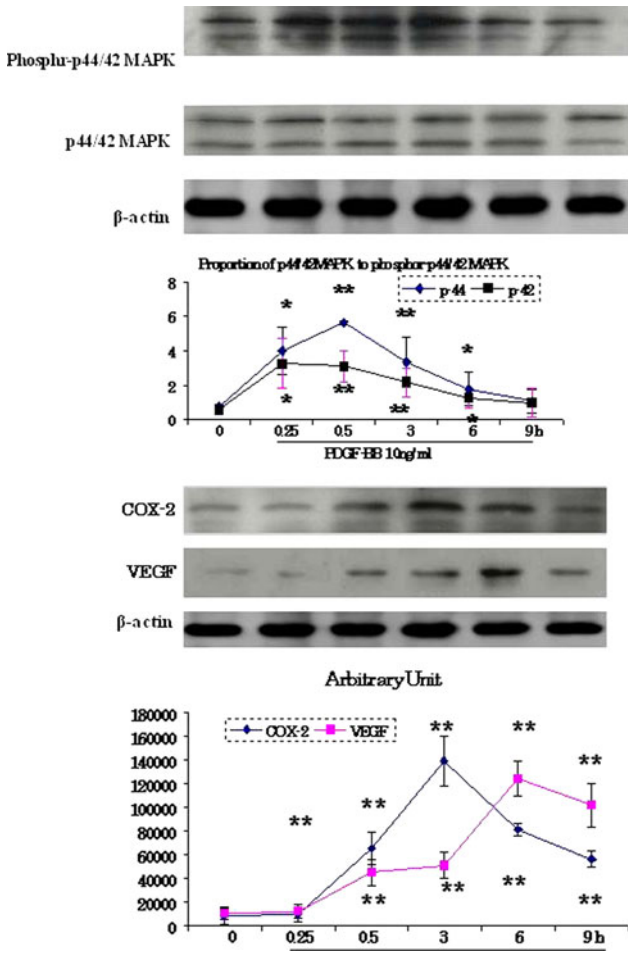

Fig. 2 PDGF induces the expression of VEGF and related molecules in activated HSCs. Activated hepatic stellate cells (HSCs) were obtained using a 1-week culture of freshly isolated HSCs in the dishes with 10% fetal bovine serum–Dulbecco's modified Eagle's medium (FBS–DMEM) and used after starvation for 24 h with 0.5% FBS–DMEM. The experiments show that PDGF-BB treatment (10 ng/mL) for 15, 30 min, 3, 6, and 9 h in serum-free DMEM. Cyclooxygenase (COX-2) protein. Phospho-mitogen-activated protein (phospho-MAPK) (*upper*) and MAPK (*lower*). Vascular endothelial growth factor (VEGF). The values show that the expression of COX-2 and phospho-MAPK were concurrently enhanced to peak at hour 3 and minute 30, respectively, preceding the VEGF peak at hour 6. Data represent mean ± SEM. $n = 3$, $^{*}P < 0.05$, $^{**}P < 0.01$ versus control

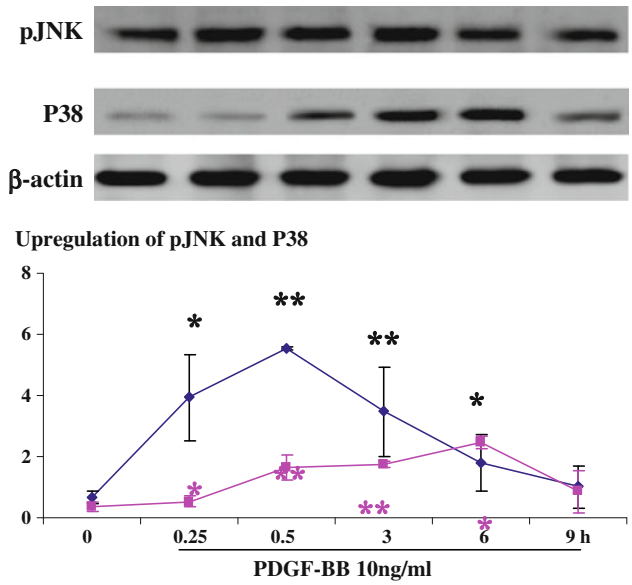

Fig. 3 PDGF induces the expression of pJNK and p38 in activated HSCs. Activated hepatic stellate cells (HSCs) were obtained through a 1-week culture of freshly isolated HSCs in the dishes with 10% fetal bovine serum–Dulbecco's modified Eagle's medium (FBS–DMEM) and used after starvation for 24 h with 0.5% FBS–DMEM. The experiments show that PDGF-BB treatment (10 ng/mL) for 15, 30 min, 3, 6, and 9 h in serum-free DMEM. c-Jun N-terminal kinase protein (pJNK) and p38 MAPK protein. The values show that expression of pJNK and p38 are concurrently enhanced up to their peak at hour 3 and minute 30, respectively. The data represent mean ± SEM. $n = 3$, $^{*}P < 0.05$, $^{**}P < 0.01$ versus control

reducing the production of VEGF protein from activated HSCs probably via COX-2/PGE2 pathway [1, 25]. COX-2 inhibitors (nimesulide and indomethacin) significantly modulated the production of VEGF in a dose- and time-dependent manner in T6-HSCs in hypoxic environment [5]. However, the exact mechanism remains to be defined.

In the present study, we demonstrated that activated HSCs produce more VEGF protein than quiescent HSCs, which indicates that activated HSCs are responsible for VEGF production, consistent with the expression of desmin and α-SMA proteins. Exogenesis PDGF-BB promotes activated HSCs to produce VEGF and COX-2 protein. However, such an event could be inhibited by pretreatment with PD98059. The suggested phospho-p44/42 MAPK expression and COX-2 production induced the activated HSCs to produce VEGF protein.

Treatment of the activated HSCs with recombinant PDGF-BB caused tyrosine phosphorylation in endogenous PDGFR-β, which activates the MAPK family to result in numerous cellular responses, including the proliferation, differentiation, and regulation of specific metabolic pathways in HSCs [25]. In injured liver models, the activated HSCs significantly expressed PDGFR-β protein and phosphor-MAPK with VEGF overexpression, which leads to angiogenesis in the healing site [17]. PDGF enhances the synthesis of cAMP to evoke growth inhibitory PG/cAMP signal, leading to the activation of COX-2 [6]. COX-2 expression induces the accumulation of hypoxia-inducible factor-1 alpha (HiF-1α) and degrades the von Hippel–Lindau (vHL) protein, which leads to VEGF production in hypoxic T6-HSCs [5].

The study shows that PDGF-BB transiently induced phospho-p44/42 MAPK expression, which peaked at min 30, and COX-2 production, which peaked at hour 3. This preceded VEGF production, with the peak at hour 6 in activated HSCs, in a time-dependent manner ($P < 0.01$;

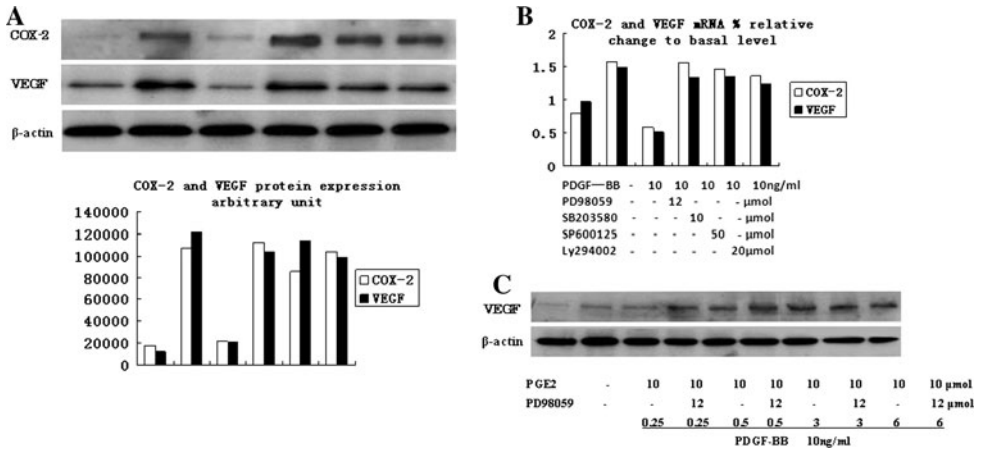

Fig. 4 PDGF-BB induces VEGF production via COX-2/PGE2 by phospho-p44/42 MAPK in the activated HSCs. COX-2 and VEGF protein in activated HSCs from 10 ng/mL PDGF-BB for 3 h, with or without pretreatment with PD98059 (12 μmol), SB203580 (10 μmol), or SP600125 (50 μmol) or Ly294002 in serum-free Dulbecco's modified Eagle's medium (DMEM) for 0.5 h were assayed by western blot analysis (**a**) and VEGF real-time quantitative PCR (**b**). Data are presented as means ± SEM. $n = 3$, $^{**}P < 0.01$ versus with PDGF-BB treatment only. Exogenous PGE_2 (10 μmol) rescued VEGF production in the PD98059-treated HSCs (**c**). Immunoblot analyses of VEGF production by the activated HSCs by PGE_2 treatment for 0.25, 0.5, 3, and 6 h, with or without pretreatment with 12 μmol of PD98059 for 0.5 h in serum-free DMEM. β-Actin was included as the internal loading control

$n = 3$). Therefore, we examined whether PDGF-induced VEGF expression by activated HSCs resulted from the MAPK signal cascade using an MEK inhibitor PD98059, a selective pharmacologic p38 MAPK inhibitor SB203580, and a selective pJNK inhibitor SP600125. MAP kinases p44 and p42 (ERK 1 and ERK 2) are praline-directed kinases activated through concomitant phosphorylation of tyrosine and threonine residues (Tyr204 and Thr202). The upstream MAP kinase regulators include MAP kinase kinase (MEK), MEK kinase, and Raf-1. JNK is phosphorylated by JNK-activating kinase and distantly related to the MAPK family, members of which are activated by dual phosphorylation at a Thr-Pro-Tyr motif, specifically at the Thr-183 and Tyr-185 residues. P38 represents a member of the MAP kinase family, with a particular feature that induces tyrosine phosphorylation of a 38-kDa protein kinase [26, 27]. The results proved that pretreatment with PD98059 suppressed PDGF-induced VEGF production and COX-2 expression in activated HSCs, but pretreatment with SB203580 and SP600125 inhibitors did not demonstrate similar inhibitory effects on VEGF or COX-2 expression. These findings suggest that p44/42 MAPK phosphorylation has a key effect on VEGF production in activated HSCs through PDGF-BB. Prostaglandins are a diverse group of autocrine and paracrine hormones that mediate many cellular and physiologic processes. In our previous report, the COX-2 is required to catalyze arachidonic acid for the synthesis of PGE_2 and subsequently induce the expression of hypoxia-inducible factor-1α that leads to the degradation of von Hippel–Lindua protein, a negative regulator of VEGF production [28]. Therefore, it is believed that the PDGF-BB induces the VEGF synthesis in activated HSCs, which is dependent on the MAPK-COX-2 signaling pathway. COX-2 catalyzes the formation of prostaglandins from arachidonic acid (AA) [28]. This can also be supported by the fact that exogenous PGE_2 could nullify the inhibitory effect of PD98059 and could rescue VEGF production in PDGF-activated HSCs, which suggests that COX-2 expression is a major approach in the event.

Conclusion

In conclusion, in injured liver, HSCs were transdifferentiated into myofibroblast-like cells, which produced VEGF protein with COX-2 overexpression. Exogenous PDGF-BB activates HSCs to produce VEGF protein by evoking COX-2 overexpression via the phospho-p44/42 MAPK pathway. Blockage of COX-2 accumulation significantly prevents VEGF production, thereby modulating hepatic fibrogenic and angiogenic events, as previously observed in experimentally induced cirrhosis.

Acknowledgments This study was supported by the Scientific and Technological Research Project of Liaoning Province (2008225009-17) and Liaoning Province Natural Science Foundation (20082058) in China.

References

1. Li D, Friedman SL (2001) Hepatic stellate cells: morphology, function, and regulation. In: The liver: biology and pathobiology, 4th edn. Raven Press, New York, pp 455–468

2. Chen SW, Zhang XR, Wang CZ, Chen WZ, Xie WF, Chen YX (2008) RNA interference targeting the platelet derived growth factor receptor beta subunit ameliorates experimental hepatic fibrosis rats. Liver Int 28:1446–1457
3. Sharma GD, Nguyen HT, Antonov AS, Gerrity RG, von Geoldern T, Pandey KN (2002) Expression of atrial natriuretic peptide receptor-A antagonizes the mitogen-activated protein kinases (Erk2 and P38MAPK) in cultured human vascular smooth muscle cells. Mol Cell Biochem 233:165–173
4. Nagineni CN, Cherukuri KS, Kutly V, Detrick B, Hooks JJ (2007) Interferon-gamma differentially regulates IGF-beta 1 and TGF beta 2 expression in human retinal pigment epithelial cells through JAK-STAT pathway. J Cell Physiol 210:192–200
5. Wang YQ, Luk JM, Ikeda K, Chu AC, Kaneda K, Fan ST (2004) Regulatory role of vHL/HIF-1α in hypoxia-induced VEGF production in hepatic stellate cells. Biochem Biophys Res Commun 317:358–362
6. Falli P, DeFranco RM, Caligiuri A, Gentilini A, Romanelli RG, Marra F, Batignani G, Guerra CT, Laffi G, Gentilini P, Pinazani M (2000) Nitrovasodilators inhibit platelet-derived growth factor-induced proliferation and migration of activated human hepatic stellate cells. Gastroenterology 119:479–492
7. Thomas KA (1996) Vascular endothelial growth factor, a potent and selective angiogenic agent. J Biol Chem 271:603–606
8. Keck PJ, Hauser SD, Krivi G, Sanzo K, Warren T, Feder J, Connolly DT (1989) Vascular permeability factor, an endothelial cell mitogen related to PDGF. Science 246:309–1312
9. Tischer E, Mitchell R, Hartman T, Silva M, Gospodarowicz D, Fiddes JC, Abraham JA (1991) The human gene for vascular endothelial growth factor. Multiple protein forms are encoded through alternative exon splicing. J Biol Chem 266:11947–11954
10. Ferrara N (1999) Vascular endothelial growth factor: molecular and biological aspects. Curr Top Microbiol Immunol 237:1–30
11. Neufeld G, Cohen T, Gengrinovitch S, Poltorak Z (1999) Vascular endothelial growth factor (VEGF) and its receptors. FASEB J 13:9–22
12. Mohle R, Green D, Moore MA, Nachman RL, Rafii S (1997) Constitutive production and thrombin-induced release of vascular endothelial growth factor by human megakaryocytes and platelets. Proc Natl Acad Sci USA 94:663–668
13. Cheng AS, Chan HL, To KF, Leung WK, Chan KK, Liew CT, Sung JJ (2004) Cyclooxygenase-2 pathway correlates with vascular endothelial growth factor expression and tumor angiogenesis in hepatitis B virus-associated hepatocellular carcinoma. Int J Oncol 24:853–860
14. Deli G, Jin CH, Mu R, Yang S, Liang Y, Chen D, Makuuchi M (2005) Immunohistochemical assessment of angiogenesis in hepatocellular carcinoma and surrounding cirrhotic liver tissues. World J Gastroenterol 11:960–963
15. Olaso E, Salado C, Egilegor E, Gutierrez V, Santisteban A, Sancho-Bru P (2003) Proangiogenic role of tumor-activated hepatic stellate cells in experimental melanoma metastasis. Hepatology 37:674–685
16. Ankoma-Sey V, Wang Y, Dai Z (2000) Hypoxic stimulation of vascular endothelial growth factor expression in activated rat hepatic stellate cells. Hepatology 31:141–148
17. Wang YQ, Ikeda K, Ikebe T, Hirakawa K, Sowa M, Nakatani K, Kawada N, Kaneda K (2000) Inhibition of hepatic stellate cell proliferation and activation by the semisynthetic analogue of fumagillin TNP-470 in rats. Hematology 32:980–989
18. Yoshiji H, Kuriyama S, Yoshii J, Ikenaka Y, Noguchi R, Hicklin DJ, Wu Y, Yanase K, Namisaki T, Yamazaki M, Tsujinoue H, Imazu H, Masaki T, Fukui H (2003) Vascular endothelial growth factor and receptor interaction is a prerequisite for murine hepatic fibrogenesis. Gut 52:1347–1354
19. Kim KY, Rhim T, Choi I, Kim SS (2001) N-acetylcysteine induces cell cycle arrest in hepatic stellate cells through its reducing activity. J Biol Chem 276:40591–40598
20. Ingber D, Fujia T, Kishimoto S, Sudo K, Kanamaru T, Brem H, Folkman J (1990) Synthetic analogues of fumagillin that inhibit angiogenesis and suppress tumour growth. Nature 348:555–557
21. Avramovich Y, Amit T, Youdim MB (2002) Non-steroidal anti-inflammatory drugs stimulate secretion of non-amyloidogenic precursor protein. J Biol Chem 277:31466–31473
22. Ikeda K, Wakahara T, Wang YQ, Kadoya H, Kawada N, Kaneda K (1999) In vitro migratory potential of rat quiescent hepatic stellate cells and its augmentation by cell activation. Hepatology 29:1760–1767
23. Ishikawa K, Mochida S, Mashiba S, Inao M, Matsui A, Ikeda H, Ohno A, Shibuya M, Fujiwara K (1999) Expressions of vascular endothelial growth factor in nonparenchymal as well as parenchymal cells in rat liver after necrosis. Biochem Biophys Res Commun 254:587–593
24. Assy N, Spira G, Paizi M (1999) Effect of vascular endothelial growth factor on hepatic regenerative activity following partial hepatectomy in rat. J Hepatol 30:911–915
25. Wang YQ, Luk JM, Chu AC, Ikeda K, Man K, Kaneda k, Fan ST (2006) TNP-470 blockage of VEGF synthesis in activated hepatic stellate cells is dependent on MAPK/COX-2-signaling pathway. Biochem Biophys Res Commun 341:239–244
26. Boulton TG, Gregory JS, Cobb MH (1991) Purification and properties of ERK 1, an insulin-stimulated MAP2 protein kinase. Biochemistry 30:278–286
27. Kyriakis JM, Banerjee P, Nikolakaki E, Dai T, Rubie EA, Ahmad MF, Avruch J, Woodgett JR (1994) The stress activated protein kinase subfamily of c-Jun kinases. Nature 369:156–160
28. Tsujii M, DuBois RN (1995) Alteration in cellular adhesion and apoptosis in epithelial cells overexpressing prostaglandin endoperoxide synthase 2. Cell 83:493–501
29. Marra F, Gentilini A, Pinzani M, Choudhury GG, Parola M, Herbst H, Dianzani MU, Laffi G, Abboud HE, Gentilini P (1997) Phosphatidylinositol 3-kinase is required for platelet-derived growth factor's actions on hepatic stellate cells. Gastroenterology 112:1297–1306
30. Reif S, Lang A, Lindquist JN, Yata Y, Gabele E, Scanga A, Brenner DA, Rippe RA (2003) The role of focal adhesion kinase-phosphatidylinositol 3-kinase-akt signaling in hepatic stellate cell proliferation and type I collagen expression. J Biol Chem 278:8083–8090